

# Compounds and subsolidus phase relations in the CaO–Co<sub>3</sub>O<sub>4</sub>–CuO system

Yuzuru Miyazaki<sup>a,\*</sup>, Xiangyang Huang<sup>b</sup>, Tsuyoshi Kajitani<sup>a</sup>

<sup>a</sup>Department of Applied Physics, Graduate School of Engineering, Tohoku University, Aramaki Aoba 6-6-05, Aoba-ku, Sendai 980-8579, Japan

<sup>b</sup>Core Research for Evolutional Science and Technology, Japan Science and Technology Agency, 3-4-15 Nihonbashi, Chuo-ku, Tokyo 103-0027, Japan

Received 23 May 2005; received in revised form 28 June 2005; accepted 30 June 2005

Available online 11 August 2005

## Abstract

We have investigated the subsolidus phase relations in the system CaO–Co<sub>3</sub>O<sub>4</sub>–CuO at 920 °C under 1 atm of oxygen by means of powder X-ray diffraction method. Apart from the three known phases of Ca<sub>2</sub>CuO<sub>3</sub>, Ca<sub>3</sub>Co<sub>2</sub>O<sub>6</sub> and (Co<sub>1-x</sub>Cu<sub>x</sub>)<sub>3</sub>O<sub>4</sub> spinel (0 ≤ x ≤ 0.06), two misfit-layered cobaltates have been identified. The first misfit is a solid solution, having a chemical formula [Ca<sub>2</sub>(Co<sub>1-x</sub>Cu<sub>x</sub>)O<sub>3</sub>]<sub>p</sub>CoO<sub>2</sub> with 0 ≤ x ≤ 0.12, while the other misfit has a pinpoint composition of [Ca<sub>2</sub>(Co<sub>0.65</sub>Cu<sub>0.35</sub>)<sub>2</sub>O<sub>4</sub>]<sub>p</sub>CoO<sub>2</sub>. Both the phases have an incommensurate *b*-axes ratio, *p* ~ 0.62, due to the size difference between the two subsystems. Another phase is found in the Cu-rich quasi-one-dimensional composite crystal Ca<sub>p</sub>(Cu<sub>1-x</sub>Co<sub>x</sub>)O<sub>2</sub> (*p* ~ 0.83, 0.08 ≤ x ≤ 0.34), but the terminal compound Ca<sub>0.83</sub>CuO<sub>2</sub> is not synthesized. The octahedral Co site in the Ca<sub>3</sub>Co<sub>2</sub>O<sub>6</sub> phase can be partially substituted with Cu, up to 6%, to form the Ca<sub>3</sub>(Co<sub>1-x</sub>Cu<sub>x</sub>)<sub>2</sub>O<sub>6</sub> (0 ≤ x ≤ 0.06) solid solution.

© 2005 Elsevier Inc. All rights reserved.

**Keywords:** Phase relations; Ca–Co–Cu–O system; Solid solution; Composite crystal; Thermoelectric compounds; Crystal structure; Rietveld analysis

## 1. Introduction

Since the discovery of large Seebeck coefficient in the layered compound  $\gamma$ -Na<sub>x</sub>CoO<sub>2</sub> [1], cobalt oxides have attracted much attention as potential thermoelectric (TE) materials. The  $\gamma$ -Na<sub>x</sub>CoO<sub>2</sub> crystal consists of an alternate stack of a highly disordered Na atoms layer and a CdI<sub>2</sub>-type CoO<sub>2</sub> conduction sheet parallel to the *c*-axis. Such an anisotropic structure is believed to be favorable to realize high TE power factor ( $S^2/\rho$ , where *S* and  $\rho$  represent the Seebeck coefficient and electric resistivity, respectively) and low thermal conductivity ( $\kappa$ ) simultaneously, necessary for good TE materials. To date, several cobaltates which possess the CoO<sub>2</sub> sheets have been reported in the Ca–Co–O [2–4], Bi–*M*–Co–O (*M* = Ca, Sr, Ba) [5,6], Tl–Sr–Co–O [7], Pb–Sr–Co–O [8] and Ca–Co–Cu–O [9] systems and all the compounds

exhibit reasonable TE properties. Analogous to the CuO<sub>2</sub> square sheet in the high-*T<sub>c</sub>* superconductors, the CoO<sub>2</sub> triangular sheet should be a prerequisite component for realizing high TE power factor.

For a practical TE material utilized at a high temperature, the volatility of constituent elements and a low decomposition temperature of the compound are serious drawbacks. The systems containing Na, Bi, Tl and Pb may not be applicable even if they exhibit excellent TE properties at around room temperature. For this reason, the cobaltates in the Ca–Co–(Cu–)O system, i.e., [Ca<sub>2</sub>CoO<sub>3</sub>]<sub>p</sub>CoO<sub>2</sub> [2–4] and [Ca<sub>2</sub>(Co<sub>0.65</sub>Cu<sub>0.35</sub>)<sub>2</sub>O<sub>4</sub>]<sub>p</sub>CoO<sub>2</sub> [9], appear to be most suitable for such TE materials. Since these compounds are crystallized in misfit-layered structures, the structure formula is represented with an irrational misfit parameter, *p*, due to the size difference between the subsystems. A higher-dimensional superspace group description is necessary to precisely represent the crystal structures and chemical compositions for above composite crystals. Besides the

\*Corresponding author. Fax: +81 22 217 7970.

E-mail address: [miya@crystal.apph.tohoku.ac.jp](mailto:miya@crystal.apph.tohoku.ac.jp) (Y. Miyazaki).

two misfit-layered cobaltates, four compounds  $\text{Ca}_3\text{Co}_2\text{O}_6$  [10],  $\text{Ca}_2\text{CuO}_3$  [11],  $\text{CaCu}_2\text{O}_3$  [12] and  $\text{Ca}_p\text{CuO}_2$  [13,14], have been reported to exist in this system at  $T > 800^\circ\text{C}$  under ambient pressure. A detailed study is thus necessary to comprehend the phase-relations, the precise stoichiometry of each phase, a possible multiple-phase range and the existence of unknown phases in the Ca–Co–Cu–O system. In this study, we have investigated the subsolidus phase-relations in the Ca–Co–Cu–O system at  $T = 920^\circ\text{C}$  and  $P_{\text{O}_2} = 1\text{ atm}$ , being considered as an optimum sintering condition for the misfit-layered cobaltates.

## 2. Experimental

Polycrystalline samples were prepared by the standard solid-state reaction method. Appropriate amounts of  $\text{CaCO}_3$  (99.99%),  $\text{Co}_3\text{O}_4$  (99.9%) and  $\text{CuO}$  (99.99%) powders were mixed in an agate mortar and pressed into pellets. The pellets were heated in a horizontal tube-type furnace at  $920^\circ\text{C}$  for 12 h in flowing oxygen (99.5%) gas with a flow rate of  $10\text{ cm}^3/\text{min}$ . Then, the samples were furnace-cooled to room temperature, ground and pelletized. Next, the pellets were heated under the identical condition. This sintering process was repeated until the homogeneous samples, being monitored by X-ray diffraction, were obtained. As the partial pressure of oxygen was kept at constant (i.e.,  $P_{\text{O}_2} = 1\text{ atm}$ ), the Ca–Co–Cu–O system can be treated as a pseudo-ternary of  $\text{CaO–Co}_3\text{O}_4\text{–CuO}$ .

X-ray diffraction (XRD) data were collected with  $\text{CuK}_\alpha$  radiation at  $25 \pm 0.5^\circ\text{C}$  in the  $2\theta$  range of  $10\text{--}100^\circ$  with  $0.040^\circ$  step using a Rigaku RAD-X diffractometer equipped with a curved graphite monochromator. The XRD data were analyzed using a Rietveld refinement program, either RIETAN-2000 [15] or PREMOS 91 [16], depending on whether the symmetry of the compounds is three dimensional (RIETAN) or modulated (PREMOS).

## 3. Results and discussion

### 3.1. Subsidiary phase relations in pseudo-binary systems

The phase compatibilities in the CaO–CuO pseudo-binary system have been extensively studied [17–20] because the system is an essential component of cuprate superconductors. Apart from the terminal compounds CaO and CuO, three compounds  $\text{Ca}_2\text{CuO}_3$  [11],  $\text{CaCu}_2\text{O}_3$  [12] and  $\text{Ca}_p\text{CuO}_2$  ( $P \sim 0.83$ ) [13,14] are known to exist at ambient pressure in this system.  $\text{Ca}_2\text{CuO}_3$  [11] crystallizes in an orthorhombic unit cell (space group  $\text{Immm}$ ) with lattice parameters of  $a = 12.239\text{ \AA}$ ,  $b = 3.779\text{ \AA}$ , and  $c = 3.259\text{ \AA}$ . The crystal structure of

the compound can be regarded as an oxygen-deficient  $\text{K}_2\text{NiF}_4$ -type structure, in which one-dimensional (1D) rows of a corner-shared  $\text{CuO}_2$  chain are running parallel to the  $b$ -axis. The second phase  $\text{CaCu}_2\text{O}_3$  [12] is built up from deformed edge-shared two-leg  $\text{Cu}_2\text{O}_3$  ladders and a layer of Ca atoms. The crystal system is orthorhombic (space group  $\text{Pmmm}$ ) with lattice parameters of  $a = 9.85\text{ \AA}$ ,  $b = 4.11\text{ \AA}$ , and  $c = 3.47\text{ \AA}$ . The compound is reported to be stable above  $950^\circ\text{C}$ . The third phase  $\text{Ca}_p\text{CuO}_2$  was originally regarded as  $\text{Ca}_{0.85}\text{CuO}_2$  [13], where the Ca atoms are randomly distributed between the edge-shared 1D  $\text{CuO}_2$  chains. Recently, its crystal structure has been reexamined [21,22] and revealed as a composite crystal, in which two monoclinic subsystems of Ca atoms and the  $\text{CuO}_2$  chains are interpenetrating each other [21]. All the atomic site is significantly modulated due to the potential interaction between the adjacent different subsystems. This compound,  $\text{Ca}_p\text{CuO}_2$ , decomposes at temperatures above  $835^\circ\text{C}$  under  $P_{\text{O}_2} = 1\text{ atm}$  [20]. In the present experiment,  $\text{Ca}_2\text{CuO}_3$  has been solely confirmed and the mixture of  $\text{Ca}_2\text{CuO}_3$  and CuO was obtained at the Cu-rich compositions.

As for the CaO– $\text{Co}_3\text{O}_4$  system,  $\text{Ca}_3\text{Co}_2\text{O}_6$  [10],  $\text{Ca}_2\text{Co}_2\text{O}_5$  [23],  $\text{CaCo}_2\text{O}_4$  [23],  $\text{Ca}_x\text{CoO}_2$  [24] and  $[\text{Ca}_2\text{CoO}_3]_p\text{CoO}_2$  [2–4] are reported to exist at ambient pressure besides the terminal compounds. The crystal structure of  $\text{Ca}_3\text{Co}_2\text{O}_6$  was recently determined using a neutron diffraction data by Hjellvåg et al. [10]. The compound crystallizes in a rhombohedral unit cell (space group  $\text{R}\bar{3}c$ ) with lattice parameters of  $a = 9.0793(7)\text{ \AA}$  and  $c = 10.381(1)\text{ \AA}$ , where numbers in parentheses represent estimated standard deviations. The structure consists of 1D chains of  $\text{CoO}_3$  polyhedra, in which a  $\text{CoO}_6$  octahedron (Co1 site) and a  $\text{CoO}_6$  trigonal prism (Co2 site) are alternately shared their faces parallel to the  $c$ -axis. Between the  $\text{CoO}_3$  chains, Ca atoms are situated with an 8-fold coordination of O atoms. The compounds  $\text{Ca}_2\text{Co}_2\text{O}_5$  and  $\text{CaCo}_2\text{O}_4$  can be prepared by the thermal decomposition of carbonate precursors  $\text{Ca}_{1-x}\text{Co}_x\text{CO}_3$  in an oxygen atmosphere at  $650$  and  $700^\circ\text{C}$ , respectively [23]. The former phase possesses the orthorhombic brownmillerite-type structure with the lattice parameters of  $a = 11.12(1)\text{ \AA}$ ,  $b = 10.74(1)\text{ \AA}$  and  $c = 7.48(1)\text{ \AA}$ , while the latter phase has a similar structure to either  $\gamma$ - or  $\beta$ - $\text{Na}_x\text{CoO}_2$  [24]. The  $\text{Ca}_x\text{CoO}_2$  phase [25] has a similar structure to  $\text{CaCo}_2\text{O}_4$  and can be prepared through an ion-exchange method using  $\text{Na}_{2x}\text{CoO}_2$  precursors; exactly a twice amount of  $\text{Na}^+$  ions is necessary to obtain ion-exchanged  $\text{Ca}_x\text{CoO}_2$  samples. Three types of structure,  $\alpha$ -,  $\beta$ - and  $\gamma$ -phases, were reported to be stable depending on the  $x$  value between  $0.25$  and  $0.50$  [25]. The misfit-layered compound  $[\text{Ca}_2\text{CoO}_3]_p\text{CoO}_2$ , known as  $\text{Ca}_3\text{Co}_4\text{O}_9$ , was first reported by Brisi and Roland in 1968, as a stoichiometric compound  $\text{Ca}_9\text{Co}_{12}\text{O}_{28}$  [26]. Recently, the detailed crystal structure has been

determined on the basis of the (3+1)-dimensional superspace group [27,28]. The structure consists of two interpenetrating subsystems of a  $\text{CoO}_2$  sheet and a distorted triple-layered rock salt (RS)-type  $\text{Ca}_2\text{CoO}_3$  block, being incommensurate parallel to the  $b$ -axis. The  $p$  parameter, defined as  $b_{\text{CoO}_2}/b_{\text{RS}}$ , nearly equals to 0.62. In the present experiment,  $\text{Ca}_3\text{Co}_2\text{O}_6$  and  $[\text{Ca}_2\text{CoO}_3]_p\text{CoO}_2$  have been confirmed to exist.

In the  $\text{Co}_3\text{O}_4$ – $\text{CuO}$  system, the solid solution, i.e.,  $(\text{Co}_{1-x}\text{Cu}_x)_3\text{O}_4$  spinel phase was confirmed while no solubility of Co for Cu was detected for CuO. A wide range of solid solution, up to  $x \sim 1/3$ , can be prepared using a thermal decomposition route of cobalt–copper hydroxide nitrate precursors, as reported by Krezhov and Konstantinov [29]. According to their structure analysis by means of neutron diffraction technique, the Cu atoms are randomly distributed among the two (tetrahedral  $A$ - and octahedral  $B$ -sites) types of Co-sites with a ratio of  $\sim 1 : 2$ . In the present study, the solubility of Cu was limited up to  $x = 0.06$  and we were unable to refine the site occupancies of the Cu atom by the X-ray structure analysis.

### 3.2. Subsolidus phase relations in the $\text{CaO}$ – $\text{Co}_3\text{O}_4$ – $\text{CuO}$ system

In Fig. 1, we show the subsolidus phase relations in the  $\text{CaO}$ – $\text{Co}_3\text{O}_4$ – $\text{CuO}$  pseudo-ternary system determined at  $920^\circ\text{C}$  and  $P_{\text{O}_2} = 1$  atm. The formation of two pseudo-ternary compounds are confirmed at point

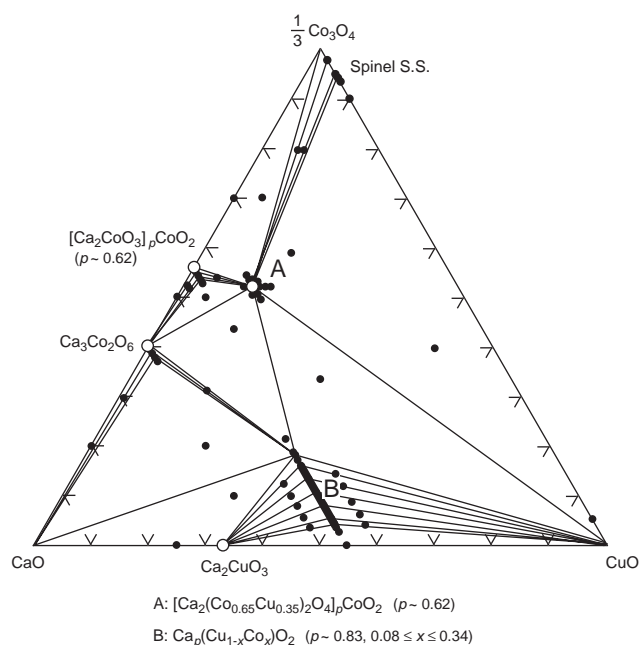


Fig. 1. Subsolidus phase relations in the  $\text{CaO}$ – $\text{Co}_3\text{O}_4$ – $\text{CuO}$  pseudo-ternary system determined at  $920^\circ\text{C}$  and  $P_{\text{O}_2} = 1$  atm. The determined compositional points are marked with closed circles.

A and line B. The point A corresponds to the composition of a misfit-layered compound  $[\text{Ca}_2(\text{Co}_{0.65}\text{Cu}_{0.35})_2\text{O}_4]_{0.62}\text{CoO}_2$  [9]. The compound has a very narrow single-phase region and no deviation of Cu:Co ratio was confirmed within the experimental errors. Fig. 2 shows the basic crystal structure of  $[\text{Ca}_2(\text{Co}_{0.65}\text{Cu}_{0.35})_2\text{O}_4]_p\text{CoO}_2$  [30]. The compound consists of a four-layered RS-type  $[\text{Ca}_2(\text{Co}_{0.65}\text{Cu}_{0.35})_2\text{O}_4]$  subsystem and the  $\text{CoO}_2$  sheet, alternately stacked perpendicular to the  $a$ – $b$  plane. On the basis of the present Rietveld analysis (XRD data), the lattice parameters were determined to be  $a = 4.8282(4)$  Å,  $b_{\text{CoO}_2} = 2.8074(7)$  Å,  $b_{\text{RS}} = 4.4930(7)$  Å,  $c = 12.785(1)$  Å and  $\beta = 93.92(1)^\circ$  at 300 K. The  $p$  value was determined to be 0.6248(4). In general, the  $\text{CdI}_2$ -type  $\text{CoO}_2$  sheet is stabilized when the formal valence state of Co ions ( $n$ ) therein is higher than +3. Then, the valence state of the RS-type subsystem (denoted as  $M$ ) should be lower than +1, i.e.,  $M^{+1-\delta}\text{Co}^{+3+\delta}\text{O}_2$ , to maintain charge balance. Without  $\text{Cu}^{2+}$  ions, the valence state of  $M$  becomes too high to maintain  $n$  as  $+3 + \delta$ . However, a large amount of  $\text{Cu}^{2+}$  would be accompanied by the creation of  $\text{Co}^{4+}$  ion (due to charge balance) with a smaller ionic radius. More than 2 Å of bond lengths are required in the  $a$ – $b$  plane of the RS-type subsystem but such long distances are quite unusual for the (Co,Cu)–O bonds, in particular if these ions take higher valence states. Hence, the small amount of  $\text{Cu}^{2+}$  ion is prerequisite for stabilizing such a four-layered block layer in the present

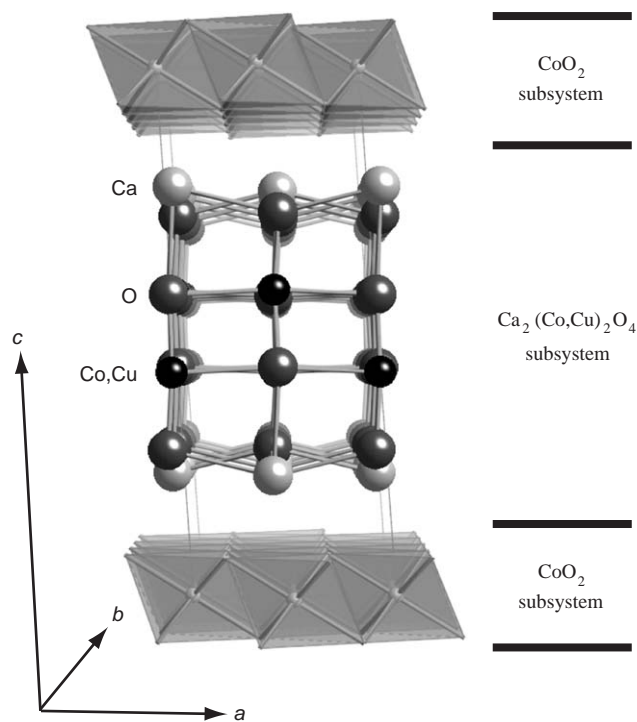


Fig. 2. Fundamental crystal structure of  $[\text{Ca}_2(\text{Co}_{0.65}\text{Cu}_{0.35})_2\text{O}_4]_p\text{CoO}_2$  viewing in perspective parallel to the  $b$ -axis [30].

compound. If we can find a suitable metallic ion with valences between 2+ and 3+ and with a larger ionic radius than that of  $\text{Cu}^{2+}$ , a similar four-layered structure with a wide compositional range can be prepared. The  $n$  value of the present compound can be evaluated as +3.15(1), on the basis of the bond valence calculation of the structure data [30]. This value is comparable to that of another misfit,  $[\text{Ca}_2\text{CoO}_3]_p\text{CoO}_2$  of  $n = +3.16(1)$  [28]. A typical polycrystalline  $[\text{Ca}_2(\text{Co}_{0.65}\text{Cu}_{0.35})_2\text{O}_4]_{0.62}\text{CoO}_2$  sample is known to exhibit  $S \sim 150 \mu\text{V K}^{-1}$  and  $\rho \sim 15 \text{ m}\Omega \text{ cm}$  at 300 K, yielding the TE power factor of  $1.5 \times 10^{-4} \text{ W K}^{-2} \text{ m}^{-1}$  [9].

Fig. 3 shows the XRD patterns ( $2\theta = 25\text{--}45^\circ$ ) of the samples with nominal composition of  $\text{Ca}_{0.83}(\text{Cu}_{1-x}\text{Co}_x)\text{O}_2$  ( $0.05 \leq x \leq 0.35$ ). The sample with  $x = 0.05$  is a mixture of the 1D cuprate solid solution  $\text{Ca}_p(\text{Cu}_{1-x}\text{Co}_x)\text{O}_2$ ,  $\text{Ca}_2\text{CuO}_3$  (closed circles) and  $\text{CuO}$  (open circles). This three-phase region was confirmed to appear for the samples with  $0 < x < 0.08$  and the solid solution was obtained on the line B with  $0.08 \leq x \leq 0.34$  (Fig. 1). Due to the superspace group symmetry, four integers  $hklm$  are necessary to index the Bragg peaks, including satellite reflections originated from the interaction between the subsystems. We assigned the  $(\text{Cu, Co})\text{O}_2$  chains to the subsystem 1 and the Ca layers to the subsystem 2. For example, the peaks indexed as

“ $hk\bar{l}0$ ” and “ $0klm$ ” are, respectively, originated from fundamental reflections of the subsystems 1 and 2, while the peaks of “ $hklm$ ” are the satellite ones. The subsystem 1 is orthorhombic while the subsystem 2 is monoclinic for the sample with  $x \leq 0.15$ . One may easily recognize that two sets of reflections belonging to the subsystem 2, “ $0kl\bar{m}$ ” and “ $0klm$ ”, become close each other with increasing  $x$  and then overlap at around  $x = 0.15$ , implying that the subsystem 2 changes from monoclinic to orthorhombic.  $\text{Ca}_3\text{Co}_2\text{O}_6$  (shown as asterisks) appears as a minor phase for the samples with  $x \geq 0.35$ . It appears that the solubility range changes with the sintering temperature. The samples with  $x = 0.35$  can be prepared by increasing sintering temperature up to  $1000^\circ\text{C}$  [31]. As for the lower  $x$  samples, the solid solution with  $0 \leq x \leq 0.30$  can be obtained at  $830^\circ\text{C}$ , just below the decomposition temperature of the terminal compound  $\text{Ca}_p\text{CuO}_2$  [32].

Table 1 summarizes the refined structural parameters of  $\text{Ca}_p(\text{Cu}_{1-x}\text{Co}_x)\text{O}_2$  samples by means of the structure analysis using a PREMOS program. The superspace group, modulation vector components  $\mathbf{k} = (p, 0, q)$  and  $wR_p$  values are also shown in the table. We adopted the superspace group  $F2/m(p0q)0s$  for the samples with  $x \leq 0.15$  and  $Fmmm(p00)0ss$  for the samples with  $x > 0.15$ . The former superspace group is equivalent to  $B2/m(\alpha\beta 0)0s$  (No. 12.2) in Table 9.8.3.5 in the literature [33]. Because of the difficulty in refining complete modulation from XRD data alone, the modulation amplitudes of each atom were not refined and the isotropic thermal displacement parameters of the O atoms,  $B_{\text{O}}$ , were fixed at 1.0. All the lattice parameter value shows continuous change with increasing  $x$ . The  $a_{(\text{Cu,Co})\text{O}_2}$ - and  $b_{(\text{Cu,Co})\text{O}_2}$ -axis lengths gradually decrease, while the  $c_{(\text{Cu,Co})\text{O}_2}$ -axis length shows an opposite tendency. The magnitude of the change (between  $x = 0.10$  and  $0.30$ ) is much significant in the  $a_{\text{Ca}}$ -axis, i.e.,  $\Delta \sim 0.045 \text{ \AA}$  (1.3%) than that of the  $c_{(\text{Cu,Co})\text{O}_2}$ -axis,  $\Delta \sim 0.022 \text{ \AA}$  (0.21%). With this large increase in  $a_{\text{Ca}}$ , the misfit parameter  $p$ , defined as  $a_{(\text{Cu,Co})\text{O}_2}/a_{\text{Ca}}$ , gradually decreases with  $x$ , from 0.8323 ( $x = 0.10$ ) to 0.8191 ( $x = 0.30$ ).

Additionally, we have confirmed that the substitution of Cu for Co is possible for the compounds  $\text{Ca}_3\text{Co}_2\text{O}_6$  and  $[\text{Ca}_2\text{CoO}_3]_p\text{CoO}_2$ . For  $\text{Ca}_3\text{Co}_2\text{O}_6$ , a partial substitution of Cu for Co was reported [34] but the solubility range was not clarified. The solubility limit of Cu in the formula,  $\text{Ca}_3(\text{Co}_{1-x}\text{Cu}_x)_2\text{O}_6$ , is determined to be  $x = 0.06$  in the present study. The sample with  $x = 0.07$  is a mixture of  $\text{Ca}_3(\text{Co, Cu})_2\text{O}_6$ ,  $\text{CaO}$  and  $\text{Ca}_p(\text{Cu, Co})\text{O}_2$  (see Fig. 1). Since there are two crystallographic sites for Co (Co1 and Co2), we determined site preference of Cu by means of the Rietveld analysis technique. Table 2 summarizes the refined structural parameters of  $\text{Ca}_3(\text{Co}_{1-x}\text{Cu}_x)_2\text{O}_6$ . The isotropic thermal displacement parameters of the O atoms,  $B_{\text{O}}$ , were fixed

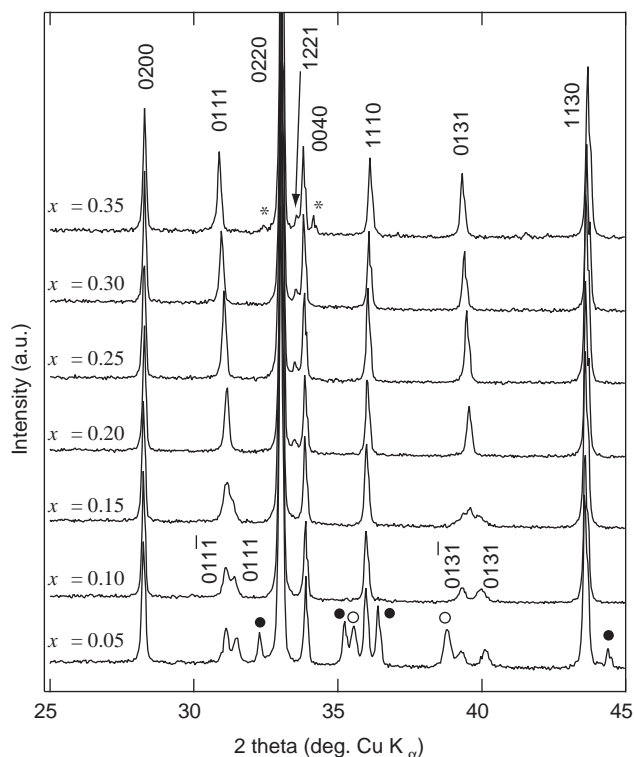


Fig. 3. Powder XRD patterns of the  $\text{Ca}_p(\text{Cu}_{1-x}\text{Co}_x)\text{O}_2$  samples with  $0.05 \leq x \leq 0.35$ . The peaks marked with asterisks, and closed and open circles are originated from  $\text{Ca}_3\text{Co}_2\text{O}_6$ ,  $\text{Ca}_2\text{CuO}_3$  and  $\text{CuO}$ , respectively.

Table 1  
Refined structural parameters of  $\text{Ca}_p(\text{Cu}_{1-x}\text{Co}_x)\text{O}_2$  by means of the Rietveld analysis

Sample	$x = 0.10$	$x = 0.15$	$x = 0.20$	$x = 0.25$	$x = 0.30$
Superspace group	$F2/m(p0q)0s$	$F2/m(p0q)0s$	$Fmmm(p00)0ss$	$Fmmm(p00)0ss$	$Fmmm(p00)0ss$
$p$	0.8323(1)	0.8295(1)	0.8267(2)	0.8233(1)	0.8191(1)
$q$	0.0528(6)	0.0106(6)	0	0	0
$wR_p$ (%)	5.62	4.49	4.40	3.66	3.46
Subsystem 1: (Cu,Co)O <sub>2</sub>					
$a$ (Å)	2.80771(7)	2.80621(8)	2.80490(7)	2.80221(9)	2.79968(7)
$b$ (Å)	6.3168(2)	6.3160(2)	6.3147(2)	6.3127(2)	6.3122(2)
$c$ (Å)	10.5820(2)	10.5860(3)	10.5921(3)	10.5960(3)	10.6041(3)
Cu/Co (0, 0, 0)					
$B_{\text{Cu}}$	2.2(2)	3.1(2)	3.0(4)	2.5(4)	2.9(4)
O ( $x_{\text{O}}, 0, z_{\text{O}}$ )					
$x_{\text{O}}$	−0.05(2)	−0.04(3)	0.05(1)	0.04(1)	0.03(1)
$z_{\text{O}}$	0.624(2)	0.623(1)	0.608(3)	0.611(3)	0.613(3)
$B_{\text{O}}^{\text{a}}$	1.0	1.0	1.0	1.0	1.0
Subsystem 2: Ca					
$a$ (Å)	3.3734(6)	3.3830(7)	3.3929(7)	3.4036(8)	3.4180(6)
$b$ (Å)	6.3168 <sup>b</sup>	6.3160 <sup>b</sup>	6.3147 <sup>b</sup>	6.3127 <sup>b</sup>	6.3122 <sup>b</sup>
$c$ (Å)	10.5835(3)	10.5861(4)	10.5921 <sup>b</sup>	10.5960 <sup>b</sup>	10.6041 <sup>b</sup>
$\beta$ (°)	90.96(1)	90.19(1)	90	90	90
Ca (0, 1/4, 1/4)					
$B_{\text{Ca}}$	2.4(4)	2.9(3)	2.7(6)	1.6(6)	2.2(7)

<sup>a</sup>Fixed at 1.0.

<sup>b</sup>The parameters are identical to those of subsystem 1.

Table 2  
Refined structural parameters of  $\text{Ca}_3(\text{Co}_{1-x}\text{Cu}_x)_2\text{O}_6$  by means of the Rietveld analysis

Parameters	Site	$x = 0$	$x = 0.02$	$x = 0.04$	$x = 0.06$
$a$ (Å)		9.0729(3)	9.0731(3)	9.0739(3)	9.0736(5)
$c$ (Å)		10.3759(2)	10.3832(3)	10.3935(3)	10.4040(4)
Ca	$8e$ ( $x_{\text{Ca}}, 0, 1/4$ )				
$x_{\text{Ca}}$		0.3694(1)	0.3695(1)	0.3693(1)	0.3690(2)
$B_{\text{Ca}}$		0.38(4)	0.54(4)	0.50(4)	0.33(5)
Co1/Cu	$6b$ (0, 0, 0)				
Co2	$6b$ (0, 0, 1/4)				
$B_{\text{Co1/Cu}} = B_{\text{Co2}}$		0.29(4)	0.49(4)	0.55(4)	0.43(5)
O	$36f$ ( $x_{\text{O}}, y_{\text{O}}, z_{\text{O}}$ )				
$x_{\text{O}}$		0.1768(3)	0.1778(3)	0.1785(4)	0.1793(5)
$y_{\text{O}}$		0.0246(4)	0.0254(4)	0.0254(4)	0.0252(5)
$z_{\text{O}}$		0.1138(3)	0.1129(3)	0.1129(3)	0.1129(3)
$B_{\text{O}}^{\text{a}}$		1.0	1.0	1.0	1.0
$wR_p$ (%)		9.36	8.72	8.49	10.19
$wR_p$ (%) <sup>b</sup>			(8.84)	(8.92)	(10.86)
$R_p$ (%)		6.39	6.27	6.26	7.68
$R_p$ (%) <sup>b</sup>			(6.34)	(6.50)	(7.96)
$R_e$ (%)		6.40	6.25	6.25	5.92

The space group of  $R\bar{3}c$  (No. 167) is adopted.

<sup>a</sup>Fixed at 1.0.

<sup>b</sup>The values for the models if the Co2 site is fully substituted with Cu.

at 1.0, in the refinement. For all the samples, we observed substantially smaller  $R$ -factors for the model in which the Co1 (octahedral) site was only substituted by

Cu; for comparison, the  $R$ -factors of the other model are shown in the brackets just below those for the adopted model. Since the  $\text{Cu}^{2+}$  ions usually prefer to sit in the

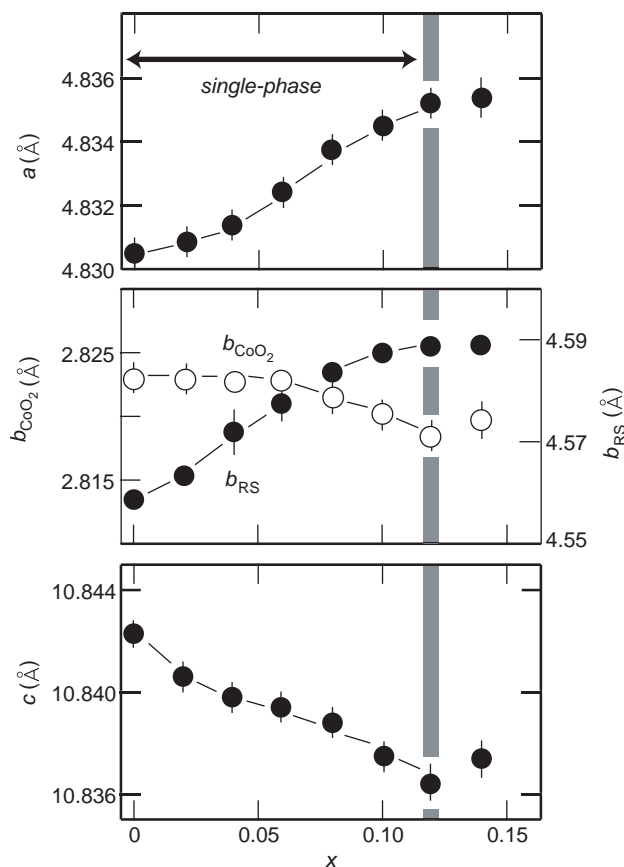


Fig. 4. Refined lattice parameters of  $[\text{Ca}_2(\text{Co}_{1-x}\text{Cu}_x)\text{O}_3]_p\text{CoO}_2$  solid solution.

octahedral coordination sites rather than the trigonal prismatic ones, the determined result is reasonable from a structural point of view. Despite of the low Cu substitution level, the  $c$ -axis length substantially increases from  $c = 10.3759(2) \text{ \AA}$  ( $x = 0$ ) to  $c = 10.4040(4) \text{ \AA}$  ( $x = 0.06$ ) with  $x$ , while the  $a$ -axis length were nearly constant from  $a = 9.0729(3) \text{ \AA}$  ( $x = 0$ ) to  $a = 9.0736(5) \text{ \AA}$  ( $x = 0.06$ ).

In the case of  $[\text{Ca}_2\text{CoO}_3]_p\text{CoO}_2$ , Cu ions are confirmed to substitute for Co ions in the RS-type subsystem. The solubility limit of Cu is determined to be  $x = 0.12$  for the  $[\text{Ca}_2(\text{Co}_{1-x}\text{Cu}_x)\text{O}_3]_p\text{CoO}_2$  solid solution. Fig. 4 shows the refined lattice parameters of the solid solution plotted against  $x$ . Reflecting the small difference in ionic radius between the Co and Cu ions, all the lattice parameter alterations were not significant except for the  $b_{\text{RS}}$ -axis length. With increasing  $x$ , the  $a$ - and  $b_{\text{RS}}$ -axis lengths linearly increase. The  $a$ -axis length gradually increases from  $4.8305(4) \text{ \AA}$  ( $x = 0$ ) to  $4.8351(5) \text{ \AA}$  ( $x = 0.12$ ) while the  $b_{\text{RS}}$ -axis shows large expansion from  $4.5587(2) \text{ \AA}$  ( $x = 0$ ) to  $4.5885(3) \text{ \AA}$  ( $x = 0.12$ ). On the other hand, the  $b_{\text{CoO}_2}$ - and  $c$ -axis lengths slightly decrease from  $2.8223(2)$  to  $2.8217(2) \text{ \AA}$  and  $10.8423(5)$  to  $10.8363(8) \text{ \AA}$ , respectively. The misfit parameter  $p$ , defined as  $b_{\text{CoO}_2}/b_{\text{RS}}$  for this compound, gradually decreased from  $0.6191(2)$  ( $x = 0$ ) to  $0.6150(2)$  ( $x =$

$0.12$ ). Although, the solubility limit is relatively low ( $x = 0.12$ ), we have observed a substantial reduction of  $\rho$  as well as an increase in  $S$  at around room temperature. The samples with  $x = 0.10$  exhibited  $\rho \sim 9 \text{ m}\Omega\text{cm}$  and  $S \sim 160 \mu\text{V K}^{-1}$  at  $300 \text{ K}$  [35]. Such an effect is ideal for increasing the TE power factor, but its origin has not been clarified yet.

In summary, we have determined the subsolidus phase relations in the  $\text{CaO}-\text{Co}_3\text{O}_4-\text{CuO}$  system at  $920^\circ\text{C}$  under 1 atm of oxygen. The system contains two misfit-layered cobaltates  $[\text{Ca}_2(\text{Co}_{1-x}\text{Cu}_x)\text{O}_3]_p\text{CoO}_2$  ( $p \sim 0.62$ ,  $0 \leq x \leq 0.12$ ) and  $[\text{Ca}_2(\text{Co}_{0.65}\text{Cu}_{0.35})_2\text{O}_4]_p\text{CoO}_2$  ( $p \sim 0.62$ ), a 1D cuprate composite crystal  $\text{Ca}_p(\text{Cu}_{1-x}\text{Co}_x)\text{O}_2$  ( $p \sim 0.83$ ,  $0.08 \leq x \leq 0.34$ ), and another two 1D compounds  $\text{Ca}_2\text{CuO}_3$  and  $\text{Ca}_3(\text{Co}_{1-x}\text{Cu}_x)_2\text{O}_6$  ( $0 \leq x \leq 0.06$ ). Apart from the thermoelectric application, the electrical and magnetic behavior of these compounds, where a mixture of Co and Cu electrons play an important role, would also be worth studying. Further experimental and theoretical studies are now in progress to understand such low-dimensional systems.

## Acknowledgments

This study was partly supported by the Core Research for Evolution Science and Technology (CREST) Project of Japan Science and Technology Agency (JST), and also by a Grant-in-Aid for Scientific Research from the Ministry of Education, Culture, Sports, Science and Technology, Japan.

## References

- [1] I. Terasaki, Y. Sasago, K. Uchinokura, Phys. Rev. B 56 (1997) R12685.
- [2] S. Li, R. Funahashi, I. Matsubara, K. Ueno, H. Yamada, J. Mater. Chem. 9 (1999) 1659.
- [3] A.C. Masset, C. Michel, A. Maignan, M. Hervieu, O. Toulemondde, F. Atuder, B. Raveau, J. Hejtmanek, Phys. Rev. B 62 (2000) 166.
- [4] Y. Miyazaki, K. Kudo, M. Akoshima, Y. Ono, Y. Koike, T. Kajitani, Jpn. J. Appl. Phys. 39 (2000) L531.
- [5] T. Itoh, T. Kawata, T. Kitajima, I. Terasaki, Proceedings of the 17th International Conference on Thermoelectrics (ICT '98), Nagoya, 1998, IEEE, Piscataway, 1999, p. 595.
- [6] H. Leligny, D. Grebille, O. Pérez, A.C. Masset, M. Hervieu, B. Raveau, Acta Crystallogr. B 56 (2000) 173.
- [7] S. Hébert, S. Lambert, D. Pelloquin, A. Maignan, Phys. Rev. B 64 (2000) 173.
- [8] D. Pelloquin, A. Maignan, S. Hébert, C. Martin, M. Hervieu, C. Michel, L.B. Wang, B. Raveau, Chem. Mater. 14 (2002) 3100.
- [9] Y. Miyazaki, T. Miura, Y. Ono, T. Kajitani, Jpn. J. Appl. Phys. 41 (2002) L849.
- [10] H. Fjellvåg, E. Gulbrandsen, S. Aasland, A. Olsen, B. Hauback, J. Solid State Chem. 124 (1996) 190.
- [11] C.L. Teske, H. Muller-Büschbaum, Z. Anorg. Allg. Chem. 379 (1970) 234.

- [12] C.L. Teske, H. Muller-Büschbaum, Z. Anorg. Allg. Chem. 370 (1969) 134.
- [13] T. Siegrist, R.S. Roth, C.J. Rawn, J.J. Ritter, Chem. Mater. 2 (1990) 192.
- [14] T.G.N. Babu, C. Greaves, Mater. Res. Bull. 26 (1991) 499.
- [15] F. Izumi, T. Ikeda, Mater. Sci. Forum. 321–324 (2000) 198.
- [16] A. Yamamoto, Acta Cryst. A 49 (1993) 831.
- [17] A.M.M. Gadalla, J. White, Trans. Brit. Ceram. Soc. 65 (1966) 181.
- [18] Y. Ikeda, Y. Oue, K. Inaba, Y. Bando, M. Takano, J. Jpn. Soc. Powder and Powder Metall. 35 (1988) 405 (in Japanese).
- [19] R.S. Roth, C.J. Rawn, J.J. Ritter, B.P. Burton, J. Am. Ceram. Soc. 72 (1989) 1545.
- [20] B.P. Burton, C.J. Rawn, R.S. Roth, N.M. Hwang, J. Res. Natl. Inst. Stand. Technol. 98 (1993) 469.
- [21] Y. Miyazaki, M. Onoda, P.P. Edwards, S. Shamoto, T. Kajitani, J. Solid State Chem. 163 (2002) 540.
- [22] M. Isobe, K. Kimoto, E. Takayama-Muromachi, J. Phys. Soc. Jpn. 71 (2002) 782.
- [23] K. Vidyasagar, J. Gopalakrishnan, C.N.R. Rao, Inorg. Chem. 23 (1984) 1206.
- [24] Y. Ono, T. Kajitani, in: K. Koumoto, I. Terasaki, N. Murayama (Eds.), Oxide Thermoelectrics, Research Signpost, Kerala, India, 2002, p. 59.
- [25] B.L. Cushing, J.B. Wiley, J. Solid State Chem. 141 (1998) 385.
- [26] C. Brisi, P. Rolando, Ann. Chim. 58 (1968) 681.
- [27] D. Grebille, S. Lambert, F. Bouree, V. Petricek, J. Appl. Cryst. 37 (2004) 823.
- [28] Y. Miyazaki, Y. Suzuki, M. Onoda, Y. Ishii, Y. Morii, T. Kajitani, Jpn. J. Appl. Phys. 43 (2004) 6252.
- [29] K. Krezhov, P. Konstantinov, Physica B 234–236 (1997) 157.
- [30] Y. Miyazaki, T. Miura, M. Onoda, M. Uchida, Y. Ishii, Y. Ono, Y. Morii, T. Kajitani, Jpn. J. Appl. Phys. 42 (2003) 7467.
- [31] S. Lambert, D. Grebille, Chem. Mater. 14 (2002) 4904.
- [32] Y. Miyazaki, J. Solid State Chem. 177 (2004) 73.
- [33] A.J.C. Wilson, E. Prince (Eds.), International Tables for Crystallography, vol. C, Kluwer, Dordrecht, 1999, p. 914.
- [34] K. Iwasaki, H. Yamane, S. Kubota, J. Takahashi, M. Shimada, J. Alloys Comp. 14 (2002) 4904.
- [35] Y. Miyazaki, Y. Suzuki, T. Miura, Y. Ono, T. Kajitani, Proceedings of the 22nd International Conference on Thermoelectrics (ICT '03), La Grande-Motte, 2003, IEEE, Piscataway, 2004, p. 203.